

Investigating Molecular Recognition by Mass Spectrometry: Characterization of Calixarene-Based Self-Assembling Capsule Hosts with Charged Guests

Christoph A. Schalley,[†] Ronald K. Castellano,^{†,‡} Marcus S. Brody,[†] Dmitry M. Rudkevich,[†] Gary Siuzdak,[†] and Julius Rebek, Jr.^{*,†}

Contribution from The Skaggs Institute for Chemical Biology and Department of Chemistry, The Scripps Research Institute, La Jolla, CA, 92037, and Department of Chemistry, Massachusetts Institute of Technology, Cambridge, Massachusetts 02139

Received January 27, 1999. Revised Manuscript Received March 22, 1999

Abstract: Capsules derived from the reversible assembly of calixarene tetraureas have been characterized by electrospray ionization mass spectrometry. Ion labeling was achieved through the encapsulation of ammonium ions as guest molecules. The gas-phase ion structure of the parent calixarene was determined by isotope pattern analysis, inclusion of labeled guests, and collision experiments. Competition experiments with different guest ions revealed a clear dependence of the encapsulation process on the size and shape of the guest ions. The formation of several different heterodimeric capsules, a covalently bridged capsule, and larger dumbbell-like aggregates containing two and three charged guests has been observed. The results parallel previous findings from NMR experiments in solution and thus support the validity of the MS method for characterization of these complexes in the gas phase.

Introduction

Over the past few years we have examined a number of concave, self-complementary molecules¹ which dimerize reversibly in organic solvents. A seam of hydrogen bonds holds together two monomeric subunits, and a container is formed which encapsulates small molecules. Extensive NMR studies have revealed many details of the encapsulation process in solution, but the detection of these complexes by mass spectrometry has been largely unsuccessful. Recently, a series of “softballs”² and a tetrameric capsule³ were characterized by ESI-MS.⁴ Quarternary ammonium ions were encapsulated instead of neutral guest molecules and served simultaneously as guests and ion labels in the gas phase. The advantage of this strategy over other ion-labeling procedures is that the seam of hydrogen bonds is preserved and no synthetic modifications of the systems are necessary. Collision experiments were consistent with complexes that have a compound-specific capsular gas-phase structure with a guest inside the cavity. This was further supported by the formation of heterodimers and the finding that

formation of these ions is sensitive to the size of the guest ion as well as the shape of the host monomers. Consequently, it is not only possible to generate, but also to study the binding properties of these capsules in the gas phase.

The study of noncovalently bound complexes by mass spectrometry has rapidly gained momentum since the introduction of electrospray ionization⁵ (ESI) as one of the softest ionization methods to date.⁶ A large number of reports have dealt with the mass spectrometric characterization of noncovalent protein/protein interactions,⁷ enzyme/substrate and enzyme/inhibitor complexes,⁸ assemblies of DNA⁹ with drugs, proteins,

(5) (a) Fenn, J. B.; Mann, M.; Meng, C. K.; Wong, S. F.; Whitehouse, C. M. *Mass Spectrom. Rev.* **1990**, *9*, 37. (b) Kebarle, P.; Tang, L. *Anal. Chem.* **1993**, *65*, 972A. (c) Gaskell, S. J. *J. Mass Spectrom.* **1997**, *32*, 677.

(6) For reviews, see: (a) Vicenti, M.; Pelizzetti, E.; Dalcanale, E.; Soncini, P. *Pure Appl. Chem.* **1993**, *65*, 1507. (b) Vicenti, M.; Minero, C.; Pelizzetti, E.; Secchi, A.; Dalcanale, E. *Pure Appl. Chem.* **1995**, *67*, 1075. (c) Vicenti, M. *J. Mass Spectrom.* **1995**, *30*, 925. (d) Przybylski, M.; Glocker, M. O. *Angew. Chem., Int. Ed. Engl.* **1996**, *35*, 806. (e) Brodbelt, J. S.; Dearden, D. V. In *Comprehensive Supramolecular Chemistry*; Atwood, J. L., Davies, J. E. D., MacNicol, D. D., Vögtle, F., Lehn, J.-M., Eds.; Pergamon Press: Oxford, 1996; Vol. 8, p 567. (f) Smith, R. D.; Bruce, J. E.; Wu, Q.; Lei, Q. P. *Chem. Soc. Rev.* **1997**, *26*, 191.

(7) (a) Smith, R. D.; Loo, J. A.; Ogorzalek-Loo, R. R.; Busman, M.; Udseth, H. R. *Mass Spectrom. Rev.* **1991**, *10*, 359. (b) Light-Wahl, K. J.; Schwartz, B. L.; Smith, R. D. *J. Am. Chem. Soc.* **1994**, *116*, 5271. (c) Kriwacki, R. W.; Wu, J.; Siuzdak, G.; Wright, P. E. *J. Am. Chem. Soc.* **1996**, *118*, 5320. (d) Loo, J. A. *Mass Spectrom. Rev.* **1997**, *16*, 1.

(8) (a) Ganem, B.; Li, Y.-T.; Henion, J. D. *J. Am. Chem. Soc.* **1991**, *113*, 6294. (b) Ganem, B.; Li, Y.-T.; Henion, J. D. *J. Am. Chem. Soc.* **1991**, *113*, 7878. (c) Cheng, X.; Chen, R.; Bruce, J. E.; Schwartz, B. L.; Anderson, G. A.; Hofstadler, S. A.; Gale, D. C.; Smith, R. D.; Gao, J.; Sigal, G. B.; Mammen, M.; Whitesides, G. M. *J. Am. Chem. Soc.* **1995**, *117*, 8859.

(9) (a) Gale, D. C.; Goodlett, D. R.; Light-Wahl, K. J.; Smith, R. D. *J. Am. Chem. Soc.* **1994**, *116*, 6027. (b) Ganem, B.; Li, Y.-T.; Hsieh, Y.-L.; Henion, J. D.; Kaboord, B. F.; Frey, M. W.; Benkovic, S. J. *J. Am. Chem. Soc.* **1994**, *116*, 1352. (c) Cheng, X.; Harms, A. C.; Goudreau, P. N.; Terwilliger, T. C.; Smith, R. D. *Proc. Natl. Acad. Sci. U.S.A.* **1996**, *93*, 7022.

[†] The Scripps Research Institute.

[‡] Massachusetts Institute of Technology.

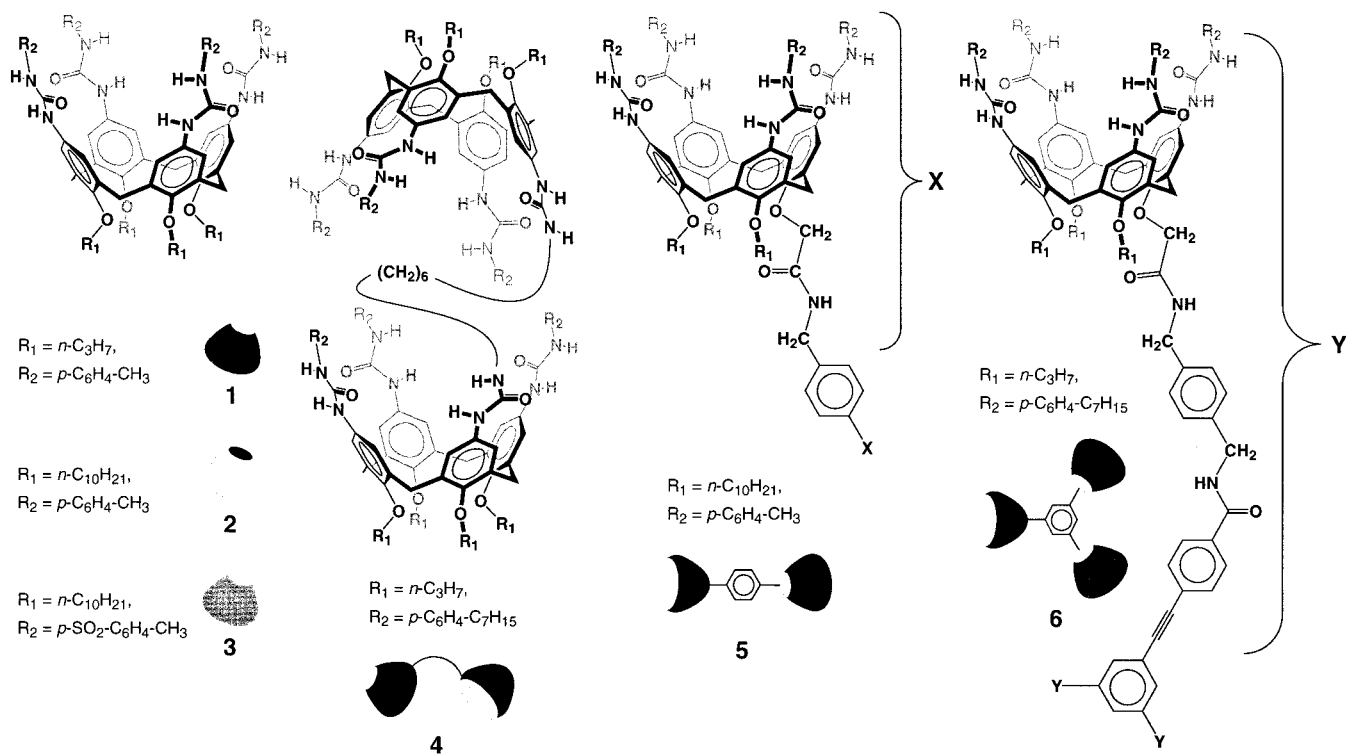
(1) (a) Rebek, J., Jr. *Chem. Soc. Rev.* **1996**, 255. (b) Conn, M. M.; Rebek, J., Jr. *Chem. Rev.* **1997**, *97*, 1647. (c) de Mendoza, J. *Chem.—Eur. J.* **1998**, *4*, 1373.

(2) (a) Branda, N.; Grotzfeld, R. M.; Valdés, C.; Rebek, J., Jr. *J. Am. Chem. Soc.* **1995**, *117*, 85. (b) Meissner, R. S.; Rebek, J., Jr.; de Mendoza, J. *Science* **1995**, *270*, 1485. (c) Meissner, R.; Garcias, X.; Mecozzi, S.; Rebek, J., Jr. *J. Am. Chem. Soc.* **1997**, *119*, 77. (d) Rivera, J. M.; Martín, T.; Rebek, J., Jr. *J. Am. Chem. Soc.* **1998**, *120*, 819. (e) Tokunaga, Y.; Rudkevich, D. M.; Santamaría, J.; Hilmersson, G.; Rebek, J., Jr. *Chem.—Eur. J.* **1998**, *4*, 1449.

(3) Martín, T.; Obst, U.; Rebek, J., Jr. *Science* **1998**, *281*, 1842.

(4) (a) Schalley, C. A.; Rivera, J. M.; Martín, T.; Santamaría, J.; Siuzdak, G.; Rebek, J., Jr. *Eur. J. Org. Chem.*, in press. (b) Schalley, C. A.; Martín, T.; Obst, U.; Rebek, J., Jr. *J. Am. Chem. Soc.* **1999**, *121*, 2133.

Chart 1



and oligonucleotides, supramolecular metal complexes,¹⁰ knots and catenanes,¹¹ carcerand/guest and cavitand/guest assemblies,^{6,12} and carbohydrate complexes.¹³ Even gas-phase micelles¹⁴ and whole viruses¹⁵ have been studied.

Given this huge body of knowledge, it seems surprising that ESI-MS has been scarcely used for the mass spectrometric characterization of hydrogen-bonded supramolecular aggregates formed from small organic building blocks.¹⁶ This may be due to the lower binding constants of these species when compared to, for example, protein/substrate complexes. Furthermore, the solvents commonly employed for ESI-MS, such as methanol and water, interfere with assemblies held together by hydrogen

bonds. The use of solvents that do not compete for hydrogen bonds¹⁷ for ESI-MS requires ion labeling of the aggregates with, for example, Na^+ /crown ether complexes,^{16a} anions,^{16b} or metal cations.^{16c}

Determining the structure of weakly bound supramolecular complexes by mass spectrometry means more than merely generating complex ions with the correct mass. In previous studies,¹⁶ evidence for the structure of the assemblies has been provided by NMR and/or X-ray experiments rather than mass spectrometric means. A recent study¹⁸ of Watson–Crick base pairing of double strand oligonucleotide anions in vacuo measures the activation energies for their dissociation and represents a milestone in this direction.

The major aim of this and our previous studies⁴ is to provide an approach to the detection and characterization of these encapsulation complexes that is complementary to and independent from the NMR experiments conducted so far. In this article, we focus on calixarene-based¹⁹ self-assembling containers²⁰ (Chart 1) which feature urea functions²¹ in their hydrogen bonding schemes (Figure 1).²² Among these structures are three monomeric calixarenes which differ in their side chains (1–3).

(10) (a) Wilson, S. R.; Yasmin, A.; Wu, Y. *J. Org. Chem.* **1992**, *57*, 6941. (b) Hopfgartner, G.; Piguët, C.; Henion, J. D.; Williams, A. F. *Helv. Chim. Acta* **1993**, *76*, 1759. (c) Leize, E.; Van Dorsselaer, A.; Kraemer, R.; Lehn, J.-M. *J. Chem. Soc., Chem. Commun.* **1993**, 990. (d) Piguët, C.; Hopfgartner, G.; Bocquet, B.; Schaad, O.; Williams, A. F. *J. Am. Chem. Soc.* **1994**, *116*, 9092. (e) Bakhtiar, R.; Chen, H.; Ogo, S.; Fish, R. H. *Chem. Commun.* **1997**, 2135. (f) Funeriu, D. P.; Lehn, J.-M.; Baum, G.; Fenske, D. *Chem.—Eur. J.* **1997**, *3*, 99. (g) Stang, P. J.; Cao, D. H.; Chen, K.; Gray, G. M.; Muddiman, D. C.; Smith, R. C. *J. Am. Chem. Soc.* **1997**, *119*, 5163. (h) Manna, J.; Kuehl, C. J.; Whiteford, J. A.; Stang, P. J.; Muddiman, D. C.; Hofstadler, S. A.; Smith, R. D. *J. Am. Chem. Soc.* **1997**, *119*, 11611. (i) Jacopozzi, P.; Dalcanele, E. *Angew. Chem., Int. Ed. Engl.* **1997**, *36*, 613.

(11) (a) Bitsch, F.; Dietrich-Buchecker, C. O.; Khemiss, A.-K.; Sauvage, J.-P.; Van Dorsselaer, A. *J. Am. Chem. Soc.* **1991**, *113*, 4023. (b) Ashton, P. R.; Brown, C. L.; Chapman, J. R.; Gallagher, R. T.; Stoddart, J. F. *Tetrahedron Lett.* **1992**, *32*, 7771. (c) Ashton, P. R.; Matthews, O. A.; Menzer, S.; Raymo, F. M.; Spencer, N.; Stoddart, J. F.; Williams, D. J. *Liebigs Ann./Recueil* **1997**, 2485.

(12) For example, see: (a) Vicenti, M.; Dalcanele, E.; Soncini, P.; Guglielmetti, G. *J. Am. Chem. Soc.* **1990**, *112*, 445. (b) Vicenti, M.; Dalcanele, E. *Proceedings of the 44th ASMS Conference on Mass Spectrometry and Allied Topics*, Portland, Oregon, 1996; p 143.

(13) (a) Lamcharfi, E.; Chuilon, S.; Kerbal, A.; Kunesch, G.; Libot, F.; Virelizier, H. *J. Mass Spectrom.* **1996**, *31*, 982. Also, see: (b) Siuzdak, G.; Ichikawa, Y.; Munoz, B.; Caulfield, T. J.; Wong, C.-H.; Nicolaou, K. C. *J. Am. Chem. Soc.* **1993**, *115*, 2877.

(14) Siuzdak, G.; Bothner, B. *Angew. Chem., Int. Ed. Engl.* **1995**, *34*, 2053.

(15) (a) Siuzdak, G.; Bothner, B.; Yeager, M.; Brugidou, C.; Fauquet, C. M.; Hoey, K.; Chang, C.-M. *Chem. Biol.* **1996**, *5*, 45. (b) Siuzdak, G. *J. Mass Spectrom.* **1998**, *33*, 203.

(16) (a) Russell, K. C.; Leize, E.; Van Dorsselaer, A.; Lehn, J.-M. *Angew. Chem., Int. Ed. Engl.* **1995**, *34*, 209. (b) Cheng, X.; Gao, Q.; Smith, R. D.; Simanek, E. E.; Mammen, M.; Whitesides, G. M. *J. Org. Chem.* **1996**, *61*, 2204. (c) Jolliffe, K. A.; Crego Calama, M.; Fokkens, R.; Nibbering, N. M. M.; Timmerman, P.; Reinhoudt, D. N. *Angew. Chem., Int. Ed.* **1998**, *37*, 1247. (d) Ma, S.; Rudkevich, D. M.; Rebek, J., Jr. *J. Am. Chem. Soc.* **1998**, *120*, 4977. (e) Scherer, M.; Sessler, J. L.; Moini, M.; Gebauer, A.; Lynch, V. *Chem.—Eur. J.* **1998**, *4*, 152.

(17) The use of noncompetitive solvents in ESI-MS studies has previously been described: (a) Katta, V.; Chowdhury, S. K.; Chait, B. T. *J. Am. Chem. Soc.* **1990**, *112*, 5348. (b) Duffin, K. L.; Henion, J. D.; Sieh, J. *J. Anal. Chem.* **1991**, *63*, 1781. (c) Libot, F.; Virelizier, H.; Froelich, O.; Bonin, M.; Quirion, J.-C.; Husson, H.-P. *Org. Mass Spectrom.* **1994**, *29*, 806. (d) Saf, R.; Mirtl, C.; Hummel, K. *Tetrahedron Lett.* **1994**, *35*, 6653. (e) Colton, R.; D'Agostino, A.; Traeger, J. C. *Mass. Spectrom. Rev.* **1995**, *14*, 79.

(18) (a) Schnier, P. D.; Klassen, J. S.; Strittmatter, E. F.; Williams, E. R. *J. Am. Chem. Soc.* **1998**, *120*, 9605. For a review on the application of MS to oligonucleotide structure analysis, see: Nordhoff, E.; Kirpekar, F.; Roepstorff, P. *Mass. Spectrom. Rev.* **1996**, *15*, 67.

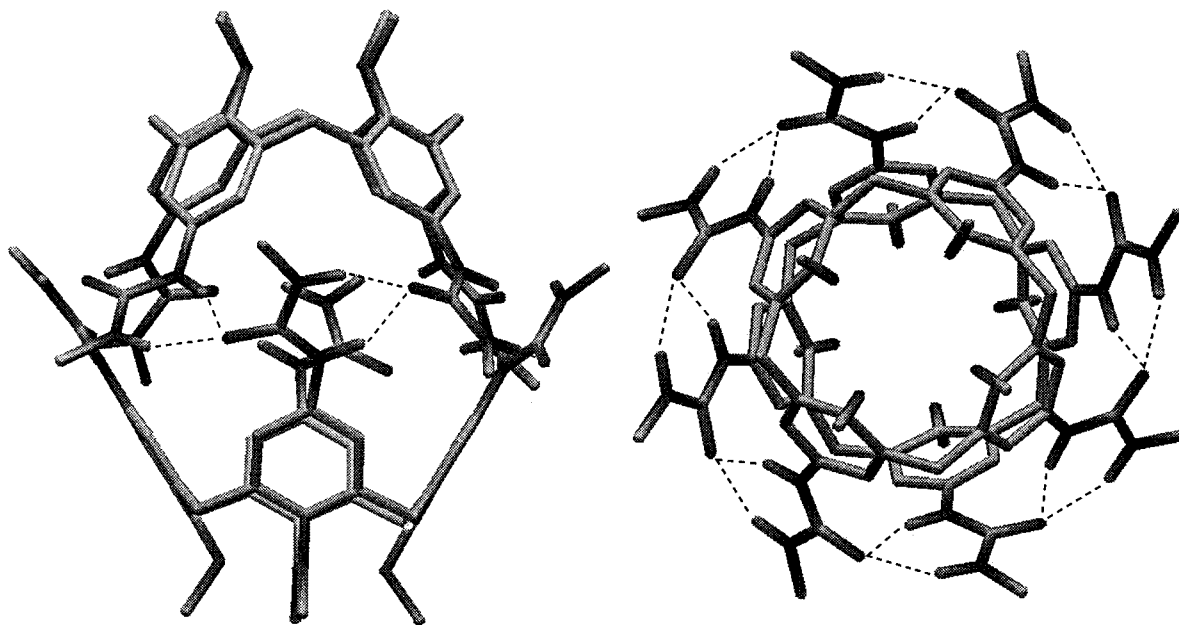


Figure 1. Side and top view of the geometry of **1•1** optimized with the Amber* force field as implemented in MacroModel 5.5.³⁰ For clarity, the side chains and carbon-centered hydrogens have been omitted.

These permit the study of heterodimer formation. Furthermore, two bridged structures are discussed, one of which, **4**, has a flexible bridge connecting the upper rims of the two halves and allows intramolecular hydrogen-bonding and the other **5**, features a rather rigid bridge between the lower rims which forbids intramolecular capsule formation. These compounds, as well as trimer **6**, provide information concerning larger aggregates containing several noncovalently bound subunits.²³

Since it is well-known that quarternary ammonium ions bind to calixarenes^{19,24,25} by cation- π interactions,^{26,27} we chose them as ionic guests (Chart 2) to provide the charge necessary for

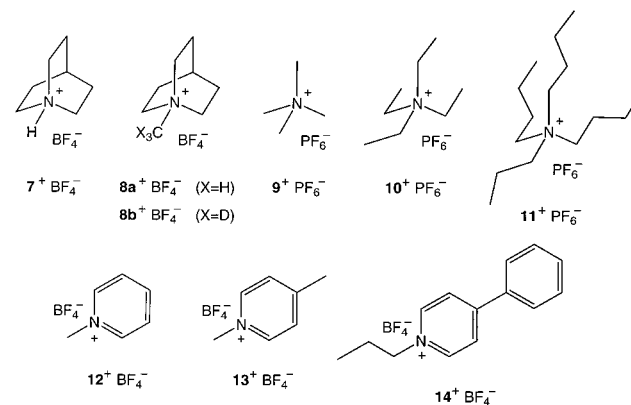
(19) For reviews on calixarene chemistry, see: (a) Gutsche, C. D. Calixarenes. In *Monographs in Supramolecular Chemistry*; Stoddart, J. F., Ed.; The Royal Society of Chemistry: Cambridge, 1989. (b) Calixarenes, a Versatile Class of Macrocyclic Compounds; Vicens, J., Böhmer, V., Eds.; Kluwer Academic: Dordrecht, 1991. (c) Böhmer, V. *Angew. Chem., Int. Ed. Engl.* **1995**, *34*, 713. (d) Ikeda, A.; Shinkai, S. *Chem. Rev.* **1997**, *97*, 1713. (e) Cram, D. J.; Cram, J. M. Container Molecules and Their Guests. In *Monographs in Supramolecular Chemistry*; Stoddart, J. F., Ed.; The Royal Society of Chemistry: Cambridge, 1994. (f) Gutsche, C. D. Calixarenes Revisited. In *Monographs in Supramolecular Chemistry*; Stoddart, J. F., Ed.; The Royal Society of Chemistry: Cambridge, 1998.

(20) For examples of hydrogen-bonded calixarene containers, see: (a) Koh, K.; Araki, K.; Shinkai, S. *Tetrahedron Lett.* **1994**, *35*, 8255. (b) Chapman, R. G.; Sherman, J. C. *J. Am. Chem. Soc.* **1995**, *117*, 9081. (c) Scheerder, J.; Vreekamp, R. H.; Engbersen, J. F. J.; Verboom, W.; Duynhoven, J. P. M.; Reinhoudt, D. N. *J. Org. Chem.* **1996**, *61*, 3476. (d) Vreekamp, R. H.; Verboom, W.; Reinhoudt, D. N. *J. Org. Chem.* **1996**, *61*, 4282. (e) MacGillivray, L. R.; Atwood, J. L. *Nature* **1997**, *389*, 469. (f) Nakamura, K.; Sheu, C.; Keating, A. E.; Houk, K. N.; Sherman, J. C.; Chapman, R. G.; Jorgensen, W. L. *J. Am. Chem. Soc.* **1997**, *119*, 4321. (g) Arduini, A.; Domiano, L.; Oglioni, L.; Pochini, A.; Secchi, A.; Ungaro, R. *J. Org. Chem.* **1998**, *62*, 77866. (h) Chapman, R. G.; Sherman, J. C. *J. Am. Chem. Soc.* **1998**, *120*, 9818.

(21) (a) Shimizu, K. D.; Rebek, J., Jr. *Proc. Natl. Acad. Sci. U.S.A.* **1995**, *92*, 12403. (b) Hamann, B. C.; Shimizu, K. D.; Rebek, J., Jr. *Angew. Chem., Int. Ed. Engl.* **1996**, *35*, 1326. (c) Mogck, O.; Böhmer, V.; Vogt, W. *Tetrahedron* **1996**, *52*, 8489. (d) Castellano, R. K.; Rudkevich, D. M.; Rebek, J., Jr. *J. Am. Chem. Soc.* **1996**, *118*, 10002. (e) Mogck, O.; Pons, M.; Böhmer, V.; Vogt, W. *J. Am. Chem. Soc.* **1997**, *119*, 5706. (f) Castellano, R. K.; Kim, B. H.; Rebek, J., Jr. *J. Am. Chem. Soc.* **1997**, *119*, 12671.

(22) For readability, the cartoons depicted in Chart 1 are used throughout this article. Different light and dark shadings are used for **1–3** to identify these compounds which differ with respect to their side chains. In addition, the following nomenclature has been employed: $[7^+@1\bullet]$ means that guest ion 7^+ is encapsulated (indicated by the "@" sign) within the dimer of calixarene **1**. In contrast, $[7^+\bullet 1]$ indicates that 7^+ and **1** form a complex with a structure which is not further specified.

Chart 2



mass spectrometric analysis. To study the effects of size and shape, these guests include bicyclic aliphatic (7^+ , $8a^+$, b^+), more flexible aliphatic (9^+ – 11^+), and aromatic (12^+ – 14^+) cations. As counterions, weakly coordinating BF_4^- and PF_6^- were chosen to increase the solubility of the salts in noncompetitive

(23) (a) Castellano, R. K.; Rudkevich, D. M.; Rebek, J., Jr. *Proc. Natl. Acad. Sci. U.S.A.* **1997**, *94*, 7132. (b) Castellano, R. K.; Rebek, J., Jr. *J. Am. Chem. Soc.* **1998**, *120*, 3657. (c) Brody, M. S.; Schalley, C. A.; Rudkevich, D. M.; Rebek, J., Jr. *Angew. Chem.*, in press.

(24) (a) Shinkai, S.; Araki, K.; Manabe, O. *J. Am. Chem. Soc.* **1988**, *110*, 7214. (b) Shinkai, S.; Araki, K.; Matsuda, T.; Nishiyama, N.; Ikeda, H.; Takasu, I.; Iwamoto, M. *J. Am. Chem. Soc.* **1990**, *112*, 9053. (c) Arnaud-Neu, F.; Fuangswasdi, S.; Notti, A.; Pappalardo, S.; Parisi, M. F. *Angew. Chem., Int. Ed.* **1998**, *37*, 112. For a review, see: (d) Lhoták, P.; Shinkai, S. *J. Phys. Org. Chem.* **1997**, *10*, 273.

(25) An X-ray structure for ammonium ions encapsulated in a calixarene container has recently been reported. See: (a) Murayama, K.; Aoki, K. *Chem. Commun.* **1998**, 607. For ammonium ions as the guests in tetrahedral M_4L_6 clusters, see: (b) Caulder, D. L.; Powers, R. E.; Parac, T. N.; Raymond, K. N. *Angew. Chem., Int. Ed.* **1998**, *37*, 1840. (c) Parac, T. N.; Caulder, D. L.; Raymond, K. N. *J. Am. Chem. Soc.* **1998**, *120*, 8003.

(26) For reviews, see: (a) Dougherty, D. A. *Science* **1996**, *271*, 163. (b) Ma, J. C.; Dougherty, D. A. *Chem. Rev.* **1997**, *97*, 1303. Also, see: Claessens, C. G.; Stoddart, J. F. *J. Phys. Org. Chem.* **1997**, *10*, 254.

(27) The interaction between ammonium ions and aromatic rings is well documented. For example, see: (a) Stauffer, D. A.; Barrans, R. E., Jr.; Dougherty, D. A. *J. Org. Chem.* **1990**, *55*, 2762. (b) Stauffer, D. A.; Dougherty, D. A. *Science* **1990**, *250*, 1558. (c) Verdonk, M. L.; Boks, G. J.; Kooijmann, H.; Kantors, J. A.; Kroon, J. J. *J. Comput.-Aided Mol. Des.* **1993**, *7*, 173. (d) Murayama, K.; Aoki, K. *Chem. Commun.* **1997**, 119.

solvents (e.g., CHCl_3) and to prevent interaction of the anions with the seam of hydrogen bonds.

Experimental Section

Syntheses. Calixarenes **3**, **4**, and **6** have been described previously.^{21f,23b,c} Calixarenes **1** and **2** were prepared from the known tetraamines²⁸ by reaction with *p*-tolyl isocyanate.^{21,23} Compound **5** was synthesized in three steps from the known tetraamine as described previously.^{23b} Ammonium salts 9^+PF_6^- – 11^+PF_6^- were used as received (Aldrich). Compound 14^+BF_4^- was prepared from its iodide (Aldrich) by anion exchange with AgBF_4 . All other ammonium salts were synthesized by reacting an ethereal solution of the corresponding amine with methyl iodide (1 equiv) and AgBF_4 (1 equiv). The mixture was stirred at room temperature for 2 h, and the salt was taken up in acetone. Filtration to remove AgI and evaporation of the solvent gave the ammonium salts in >95% yield. The salts were further purified by recrystallization from CH_2Cl_2 by the slow infusion of hexane.

Proton (^1H) and carbon (^{13}C) NMR spectra were recorded on a Bruker DRX-600 (600 and 151 MHz, respectively) spectrometer. IR spectra were recorded on a Perkin-Elmer Paragon 1000PC FT-IR spectrometer. Fast atom bombardment (FAB) positive ion mass spectra were obtained on a VG ZAB-VSE double-focusing high-resolution mass spectrometer equipped with a cesium ion gun. Routine electrospray ionization (ESI) mass spectrometry experiments were performed on an API III Perkin-Elmer SCIEX triple quadrupole mass spectrometer.

5,11,17,23-Tetrakis(tolylurea)-25,26,27,28-tetrakis(propoxy) calix-[4]arene (1): ^1H NMR (300 MHz, CDCl_3) δ (ppm) = 9.32 (s, 4H), 7.72 (d, J = 8.2 Hz, 8H), 7.65 (d, 4H, J = 2.0 Hz), 7.12 (d, 8H, J = 8.2 Hz), 7.01 (s, 4H), 5.89 (d, 4H, J = 2.0 Hz), 4.24 (d, 4H, J = 13.0 Hz), 3.65 (t, 8H, J = 7.0 Hz), 2.81 (d, 4H, J = 13.0 Hz), 2.26 (s, 12H), 1.90 (m, 8H), 0.95 (t, 12H, J = 7.0 Hz). ^{13}C NMR (300 MHz, $\text{DMSO}-d_6$) δ (ppm) = 8.23 (s, 4H), 8.16 (s, 4H), 7.22 (d, 8H, J = 8.2 Hz), 7.04 (d, 8H, J = 8.2 Hz), 6.81 (s, 8H), 4.33 (d, 4H, J = 12.9 Hz), 3.78 (t, 8H, J = 7.2 Hz), 3.09 (d, 4H, J = 12.9 Hz), 2.20 (s, 12H), 1.90 (m, 8H), 1.00 (t, 12H, J = 7.2 Hz). ^{13}C NMR (151 MHz, $\text{DMSO}-d_6$) δ (ppm) = 153.33, 151.85, 138.13, 135.20, 134.32, 131.07, 129.91, 119.02, 118.83, 77.33, 31.47, 23.50, 21.16, 11.07. IR (thin film) 3386, 2957, 2919, 2871, 1664, 1602, 1550, 1514, 1467, 1314 cm^{-1} . HRMS (FAB, $\text{M} + \text{Cs}^+$) calcd for $\text{C}_{72}\text{H}_{80}\text{N}_8\text{O}_8\text{Cs}^+$ 1317.5153, found 1317.5104.

5,11,17,23-Tetrakis(tolylurea)-25,26,27,28-tetrakis(decyloxy) calix-[4]arene (2): ^1H NMR (600 MHz, $\text{DMF}-d_7$) δ (ppm) = 8.39 (s, 4H), 8.32 (s, 4H), 7.34 (d, 8H, J = 8.3 Hz), 7.08 (d, 8H, J = 8.4 Hz), 6.91 (s, 8H), 4.46 (d, 4H, J = 13.0 Hz), 3.92 (t, 8H, J = 7.2 Hz), 3.15 (d, 4H, J = 13.2 Hz), 2.25 (s, 12H), 1.99 (m, 8H), 1.51–1.33 (m, 56H), 0.92 (t, 12H, J = 7.1 Hz). ^{13}C NMR (151 MHz, $\text{DMF}-d_7$) δ (ppm) = 153.26, 152.03, 138.33, 135.19, 134.35, 130.79, 129.39, 119.02, 118.36, 75.44, 32.26, 31.38, 30.70, 30.53, 30.48, 30.23, 29.79, 26.92, 22.92, 20.22, 14.03. IR (thin film) 3338, 2923, 2853, 1666, 1604, 1553, 1514, 1469, 1315, 1213, 816 cm^{-1} . HRMS (FAB; $\text{M} + \text{Cs}^+$) calcd for $\text{C}_{100}\text{H}_{136}\text{N}_8\text{O}_8\text{Cs}^+$ 1709.9535, found 1709.9598.

5,11,17,23-Tetrakis(tolylurea)-25,26,27-tris(decyloxy)-28-[(ethoxy-carbonyl)methoxy] calix[4]arene: ^1H NMR (600 MHz, $\text{DMF}-d_7$) δ (ppm) = 8.48 (s, 1H), 8.47 (s, 1H), 8.45 (s, 1H), 8.43 (s, 1H), 8.33 (s, 2H), 8.26 (s, 2H), 7.39 (d, 4H, J = 8.3 Hz), 7.30 (d, 4H, J = 8.4 Hz), 7.11–7.06 (m, 12H), 6.76 (s, 4H), 4.82 (s, 2H), 4.70 (d, 2H, J = 13.3 Hz), 4.47 (d, 2H, J = 13.0 Hz), 4.23 (q, 2H, J = 7.1 Hz), 3.93 (m, 2H), 3.90 (m, 2H), 3.82 (m, 2H), 3.19 (d, 2H, J = 13.7 Hz), 3.16 (d, 2H, J = 13.3 Hz), 2.26 (s, 6H), 2.25 (s, 6H), 2.02 (m, 2H), 1.96 (m, 4H), 1.55–1.30 (m, 45H), 0.92–0.89 (m, 9H). ^{13}C NMR (151 MHz, $\text{DMF}-d_7$) δ (ppm) = 170.57, 153.50, 153.44, 152.58, 151.98, 151.71, 138.55, 138.48, 138.46, 135.98, 135.83, 135.06, 134.80, 134.73, 134.72, 134.57, 131.13, 131.10, 130.89, 129.63, 129.53, 119.20, 119.15, 119.12, 118.65, 118.63, 118.43, 75.67, 75.63, 71.02, 60.42, 32.20, 32.18, 31.76, 31.31, 30.62, 30.56, 30.40, 30.34, 30.29, 30.24, 30.17, 30.06, 30.04, 29.70, 29.67, 26.81, 26.62, 22.85, 20.21, 20.19, 14.22, 13.96. IR (thin film) 3339, 2924, 2853, 1764, 1736, 1666, 1605, 1553, 1514, 1473,

1316, 1216, 816 cm^{-1} . HRMS (FAB; $\text{M} + \text{Cs}^+$) calcd for $\text{C}_{94}\text{H}_{122}\text{N}_8\text{O}_{10}\text{Cs}^+$ 1655.8338, found 1655.8430.

5,11,17,23-Tetrakis(tolylurea)-25,26,27-tris(decyloxy)-28-(carboxymethoxy) calix[4]arene: ^1H NMR (600 MHz, $\text{DMF}-d_7$) δ (ppm) = 12.56 (s, 1H), 8.46 (s, 1H), 8.45 (s, 1H), 8.44 (s, 1H), 8.41 (s, 1H), 8.36 (s, 2H), 8.31 (s, 2H), 7.38 (d, 4H, J = 8.3 Hz), 7.32 (d, 4H, J = 8.3 Hz), 7.10–7.07 (m, 8H), 7.04 (s, 4H), 6.89 (m, 2H), 6.88 (m, 2H), 4.72 (s, 2H), 4.63 (d, 2H, J = 13.1 Hz), 4.49 (d, 2H, J = 12.9 Hz), 3.95 (m, 4H), 3.87 (m, 2H), 3.21 (d, 2H, J = 13.4 Hz), 3.16 (d, 2H, J = 13.1 Hz), 2.26 (s, 6H), 2.25 (s, 6H), 2.00 (m, 6H), 1.49–1.31 (m, 42H), 0.91–0.89 (m, 9H). ^{13}C NMR (151 MHz, $\text{DMF}-d_7$) δ (ppm) = 171.48, 153.50, 153.48, 153.45, 152.28, 151.78, 151.44, 139.83, 138.50, 138.45, 135.72, 135.44, 135.26, 135.16, 134.93, 134.81, 134.74, 131.11, 131.06, 130.99, 129.61, 129.56, 119.24, 119.22, 119.16, 118.62, 118.60, 118.53, 75.90, 75.82, 71.34, 32.20, 32.18, 31.70, 31.31, 30.46, 30.42, 30.36, 30.23, 30.19, 30.17, 30.15, 30.03, 29.96, 29.67, 26.65, 26.57, 22.84, 20.19, 13.97. IR (thin film) 3360, 2924, 2854, 1761, 1666, 1606, 1555, 1514, 1478, 1313, 1217, 815 cm^{-1} . HRMS (FAB; $\text{M} + \text{Cs}^+$) calcd for $\text{C}_{92}\text{H}_{118}\text{N}_8\text{O}_{10}\text{Cs}^+$ 1627.8025, found 1627.8119.

1,4-Bis(5,11,17,23-tetrakis(tolylurea)-25,26,27-tris(decyloxy)-28-[(aminocarbonyl)methoxy] calix[4]arene)xylylene (5): ^1H NMR (600 MHz, $\text{DMF}-d_7$) δ (ppm) = 8.73 (t, 2H, J = 5.8 Hz), 8.48 (s, 2H), 8.46 (s, 2H), 8.46 (s, 2H), 8.42 (s, 2H), 8.34 (s, 4H), 8.32 (s, 4H), 7.42 (s, 4H), 7.37 (d, 8H, J = 8.2 Hz), 7.30 (d, 8H, J = 8.4), 7.09 (d, 8H, J = 8.2 Hz), 7.07 (d, 8H, J = 8.5 Hz), 7.06–7.05 (m, 8H), 6.78 (s, 4H), 6.77 (s, 4H), 4.73 (s, 4H), 4.70 (d, 4H, J = 5.8 Hz), 4.52 (d, 4H, J = 13.4 Hz), 4.45 (d, 4H, J = 13.1 Hz), 3.92–3.83 (m, 12H), 3.22 (d, 4H, J = 13.7 Hz), 3.17 (d, 4H, J = 13.4 Hz), 2.26 (s, 6H), 2.26 (s, 6H), 2.25 (s, 12H), 1.91 (m, 4H), 1.81 (m, 8H), 1.42–1.31 (m, 84H), 0.91–0.88 (m, 18H). ^{13}C NMR (151 MHz, $\text{DMF}-d_7$) δ (ppm) = 169.82, 153.27, 153.22, 152.39, 151.82, 151.23, 138.60, 138.31, 138.27, 138.23, 135.75, 134.93, 134.89, 134.65, 134.57, 134.54, 134.27, 130.93, 130.90, 130.74, 129.43, 129.36, 127.51, 119.34, 119.15, 119.00, 118.93, 118.45, 118.28, 75.87, 75.12, 74.78, 42.40, 32.21, 31.86, 31.60, 30.41, 30.22, 30.17, 30.13, 30.12, 30.00, 29.69, 26.55, 26.45, 22.89, 20.23, 20.21, 14.06. IR (thin film) 3355, 2924, 2854, 1667, 1607, 1557, 1515, 1476, 1317, 1213, 815 cm^{-1} . LRMS (ESI; M_{av}) calcd for $\text{C}_{192}\text{H}_{244}\text{N}_{18}\text{O}_{18}$ 3092, found 3092.

MS Experiments. The ESI-MS experiments were performed on a single quadrupole Perkin-Elmer API-100 Sciex (mass range < 3000 amu) and a Finnigan MAT LCQ ion trap instrument (mass range < 4000 amu). The samples were introduced as 50 μM solutions of the calixarene monomers with 1.5 equiv (5–15 equiv for multiply charged species) of the guest salt in CHCl_3 at flow rates of 4–6 $\mu\text{L}/\text{min}$. The ion intensities increased with the ion spray and the orifice potentials, which were set to 4–5 kV and 100–200 V, respectively. To improve the signal-to-noise ratio, 20–50 scans were accumulated. Due to the lower mass resolution of the LCQ ion trap instrument, meaningful isotope patterns could only be recorded on the API-100 quadrupole mass spectrometer for complexes with masses lower than 3000 amu.

For guest competition experiments 50 μM solutions of calixarene **1** in CHCl_3 with 1 equiv of each guest salt were prepared. These experiments were performed with the API-100 instrument (ion spray and orifice potentials set to 5000 and 150 V, respectively), and at least 50 scans were averaged.

Collision (source-CID) experiments^{13b,29} were carried out with the LCQ mass spectrometer in the region between the skimmer and the octapole. For collision-induced decay (CID) the potential of the octapole was set to voltages between 0 and –100 V, relative to the grounded skimmer. The solvent or air molecules present in this region provided the collision gas. With these features, the instrument allows for the tuning of the collision energy that is imparted to the ions. It should be noted that all ions produced in the ion source are subjected to the same collision conditions in these experiments. The collision experiments were repeated at several different concentrations of the guest. Although the relative intensities of $[\mathbf{8a}^+\bullet\mathbf{1}]$ and $[\mathbf{8a}^+\text{@}\mathbf{1}\bullet\mathbf{1}]$ were dependent on the amount of guest added, the overall pattern which emerged upon

(28) (a) Mislin, G.; Graf, E.; Hosseini, M. W. *Tetrahedron Lett.* **1996**, 37, 4503. (b) Jakobi, R. A.; Böhmer, V.; Grüttnner, C.; Kraft, D.; Vogt, W. *New J. Chem.* **1996**, 20, 493.

(29) *Electrospray Ionization Mass Spectrometry*; Cole, R. B., Ed.; Wiley: New York, 1997.

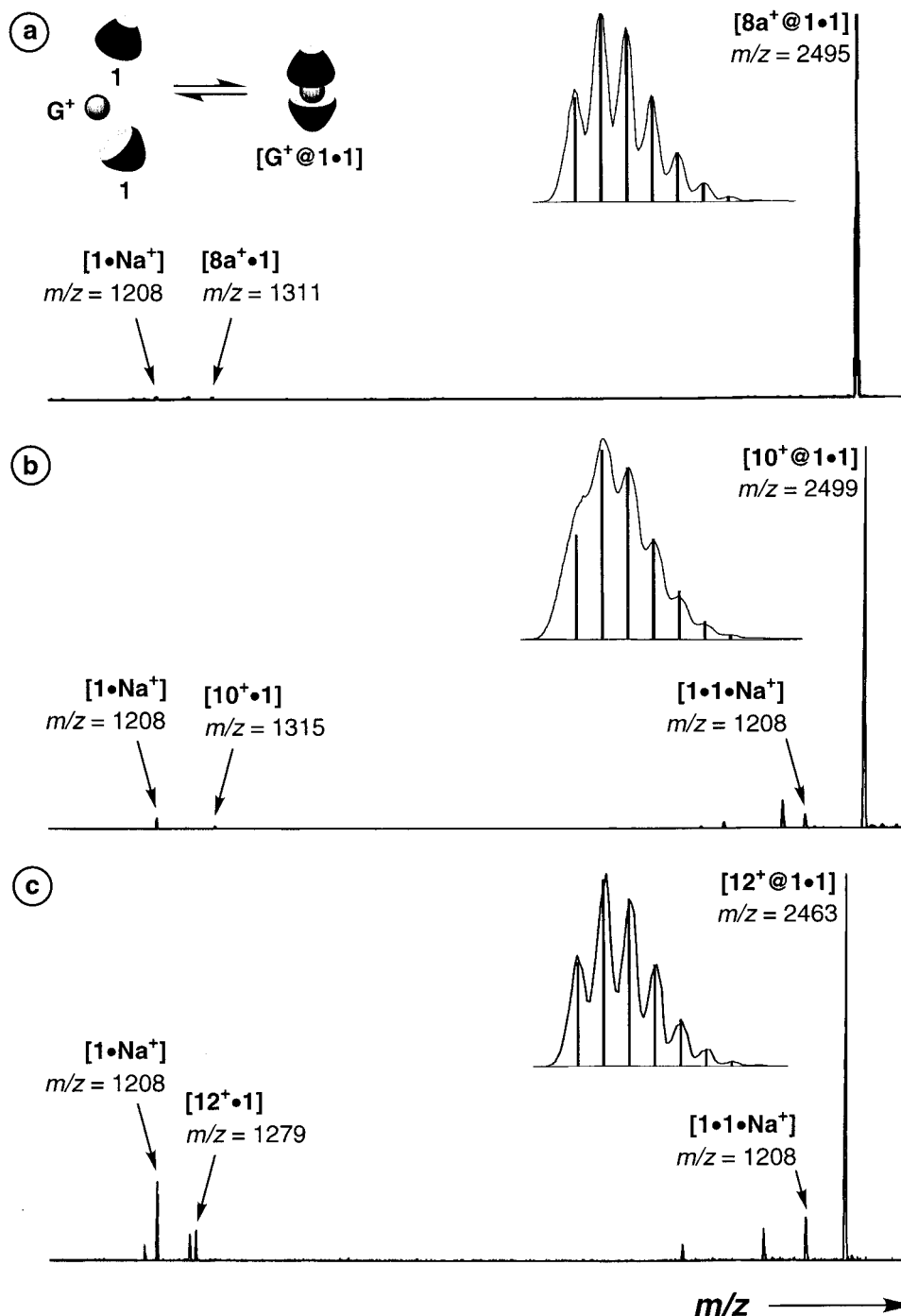


Figure 2. ESI mass spectra of CHCl_3 solutions of **1** ($50 \mu\text{M}$) with (a) $8\text{a}^+ \text{BF}_4^-$, (b) 10^+BF_4^- , and (c) 12^+BF_4^- ($75 \mu\text{M}$ each). The insets show the calculated (straight lines) and experimental isotope patterns (curves).

scanning the collision energy (see below) was reproducible. The minima, maxima, and the points of inflection of the curve shown in Figure 3 are located at the same octapole voltages in all of these experiments.

Computational Details. The geometries of the empty capsule **1•1** and guests $7^+ - 14^+$ were optimized using the Amber* force field as implemented in the MacroModel 5.5 program.³⁰ The calculations of the volumes of the cavity and the guests were performed with the GRASP program³¹ as described in detail previously.³² Briefly, the

calculation of the cavity volume involves rolling a spherical probe along the interior surface. A small probe can easily fall out of the holes, while a large probe fails to define the smaller dimples of the concave inner surface. The default size of the probe in the GRASP software package (1.4 \AA radius) is suitable. It has also been used for the calculation of other capsule volumes before and thus ensures comparability with earlier results.³² The volumes of the guests were determined as those enclosed by their van der Waals molecular surfaces.

Results and Discussion

Host–Guest Complexes of **1•1 and Their Gas-Phase Ion Structure.** Figure 2 shows the ESI mass spectra ($1000 - 2600 \text{ amu}$) of the calixarene **1** with 8a^+ , 10^+ , and 12^+ as guest ions. The base peaks correspond to the m/z values expected for

(30) (a) Mohamadi, F.; Richards, N. G.; Guida, W. C.; Liskamp, R.; Caufield, C.; Chang, G.; Hendrickson, T.; Still, W. C. *J. Comput. Chem.* **1990**, *11*, 440. (b) McDonald, D. Q.; Still, W. C. *Tetrahedron Lett.* **1992**, *33*, 7743.

(31) Nicholls, A.; Sharp, K. A.; Honig, B. *Proteins* **1991**, *11*, 281.

(32) Mecozzi, S.; Rebek, J., Jr. *Chem.–Eur. J.* **1998**, *4*, 1016.

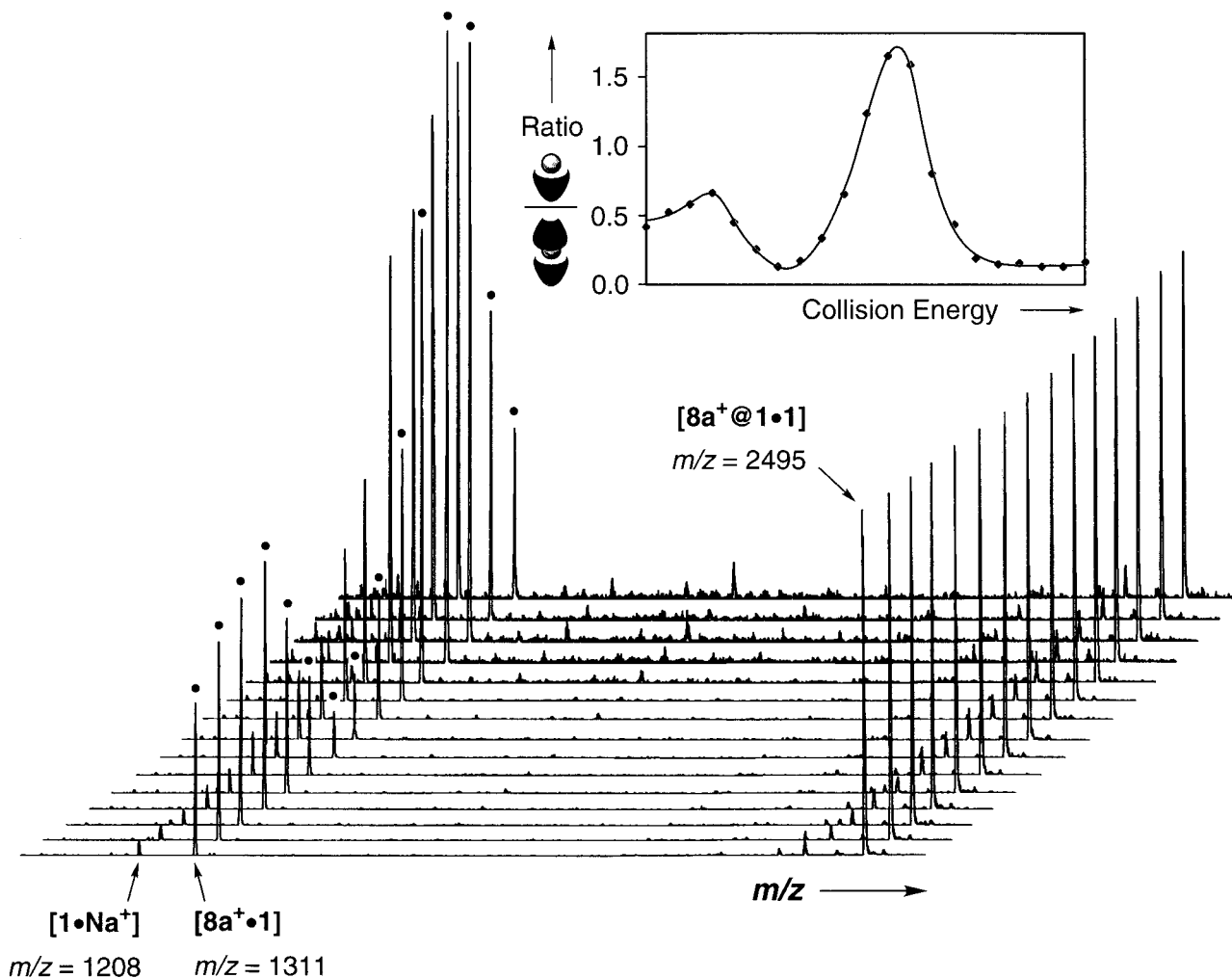


Figure 3. Electrospray mass spectra of a CHCl_3 solution of **1** ($50 \mu\text{M}$) with $8\text{a}^+ \text{BF}_4^-$ ($250 \mu\text{M}$). The spectra were recorded at octapole voltages of 0 (front) to -70 V (back) in steps of 5 V and are shown with the peak height of $[8\text{a}^+@1\bullet1]$ kept constant. For clarity, the signals for $[8\text{a}^+\bullet1]$ are labeled with dots (\bullet). The inset shows the dependence of the $[8\text{a}^+\bullet1]:[8\text{a}^+@1\bullet1]$ ratio on the collision energy (octapole voltages 0 to -100 V).

complexes of two calixarene monomers and one guest cation, i.e., $[8\text{a}^+@1\bullet1]$ ($m/z = 2495$), $[10^+@1\bullet1]$ ($m/z = 2499$), and $[12^+@1\bullet1]$ ($m/z = 2463$). Minor signals are observed for complexes of monomer and dimer with background Na^+ and monomer–guest ions $[8\text{a}^+\bullet1]$ ($m/z = 1311$), $[10^+\bullet1]$ ($m/z = 1315$), and $[12^+\bullet1]$ ($m/z = 1279$). The measured isotope patterns for $[G^+@1\bullet1]$ match those calculated on the basis of natural isotope abundances. The distance of $\Delta m = 1 \text{ amu}$ between two vicinal isotope peaks confirms the singly charged state of the ions. Together with this information, a mass shift of $\Delta m = 3 \text{ amu}$ upon replacement of 8a^+ by isotopically labeled 8b^+ confirms the presence of one guest cation and two calixarene monomers. Finally, upon addition of ca. 10% methanol as a competitive solvent the spectrum changes dramatically. The signal for $[8\text{a}^+@1\bullet1]$ vanishes completely. The base peak now corresponds to the protonated capsule monomer $[1\bullet\text{H}^+]$. Similarly, addition of dimethyl sulfoxide destroys the capsule. Only $[1\bullet\text{Na}^+]$ is observed with low intensity due to background Na^+ . From these findings, it becomes clear that $[8\text{a}^+@1\bullet1]$ is held together by hydrogen bonds. However, the gas-phase structure is not obvious from these experiments alone. Other structures have to be taken into consideration as well, for example, two monomers of **1** bound with their aromatic rings to a central ammonium ion by cation– π interactions.^{26,27} Alternatively, hydrogen-bound capsules with cations attached to their outer surfaces are conceivable. These structures differ from the host–

guest assembly not only with respect to their structural features but also in their energy threshold for fragmentation. Complexes bound only by weak forces (e.g., cation– π interactions) should fragment much more easily than the corresponding complexes where the guest is held tightly within the cavity of a complex having multiple hydrogen bonds.³³ This difference should render the structures distinguishable by mass spectrometric means.

The determination of gas-phase ion structures by mass spectrometry is, necessarily, indirect. Often, collision experiments are used to induce fragmentations that are indicative of a certain structure.^{13b,29} It was recently shown that cleavage of covalent bonds at high collision energies compete to a certain extent with the release of the guest from the dimeric “softballs”,⁴ but this competition was not observed for the monomer–guest complexes. In other words, there is a higher energy demand for the expulsion of a guest encapsulated within a dimer, with which bond cleavage can compete. The monomer–guest complex, however, releases the guest at a much lower energy threshold so that covalent bond cleavage cannot compete. Similar experiments were performed with $[8\text{a}^+@1\bullet1]$. To use the $[8\text{a}^+\bullet1]$ signal as a reference, its intensity was increased by the addition of a larger excess of the guest. Figure 3 show a series of spectra of a $50 \mu\text{M}$ CHCl_3 solution of **1** with 5 equiv

(33) In this context, it is important to note that the bond dissociation energy of hydrogen bonds is usually higher in the gas phase due to the lack of solvent competition.

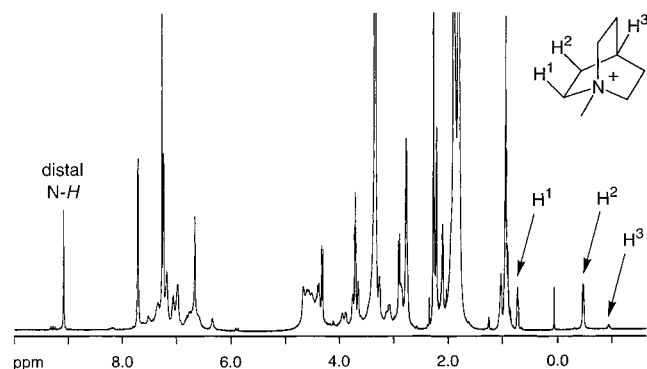
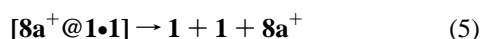
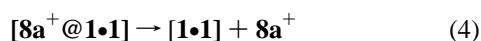


Figure 4. ^1H NMR spectra (CHCl_3 , 600 MHz) of **1** (ca. 1 mM) with $8\text{a}^+ \text{BF}_4^-$ as the guest salt (ca. 1.5 mM).

of 8a^+ added at different collision energies. Unexpectedly, even at the highest possible collision energies, no bond cleavages were observed. Instead, upon scanning the collision energy through the whole available range, a distinct pattern was found for the $[8\text{a}^+\bullet\mathbf{1}]:[8\text{a}^+\text{@}\mathbf{1}\bullet\mathbf{1}]$ ratio (inset in Figure 3). Four stages can be distinguished: (i) A slight increase of the monomer relative to the dimer at the lowest collision energies implies that $[1\bullet 8\text{a}^+]$ must be formed from a larger species, most likely by decay of a minor fraction of unspecifically bound $[1\bullet\mathbf{1}\bullet 8\text{a}^+]$ (eq 1). (ii) At slightly higher collision energies, the $[8\text{a}^+\bullet\mathbf{1}]:[8\text{a}^+\text{@}\mathbf{1}\bullet\mathbf{1}]$ ratio drops significantly to ca. 0.2, indicating that decomposition of the monomer–guest complex $[8\text{a}^+\bullet\mathbf{1}]$ into its components becomes feasible (eq 2). (iii) At even higher energies, a steep increase of the $[8\text{a}^+\bullet\mathbf{1}]:[8\text{a}^+\text{@}\mathbf{1}\bullet\mathbf{1}]$ ratio to ca. 1.8 is observed. The capsule-like dimer starts to break, reforming $[8\text{a}^+\bullet\mathbf{1}]$ at the expense of $[8\text{a}^+\text{@}\mathbf{1}\bullet\mathbf{1}]$ (eq 3). Alternatively, guest release from the capsule may occur with concomitant decrease of the $[8\text{a}^+\text{@}\mathbf{1}\bullet\mathbf{1}]$ intensity (eq 4). (iv) Finally, the collision energy is high enough to completely scatter the $[8\text{a}^+\text{@}\mathbf{1}\bullet\mathbf{1}]$ ions into the two monomers and the guest (eqs 2 and 5). The $[8\text{a}^+\bullet\mathbf{1}]:[8\text{a}^+\text{@}\mathbf{1}\bullet\mathbf{1}]$ ratio drops again to ca. 0.2 and remains essentially constant at higher collision energies. Assuming that the $\mathbf{1}\text{--Na}^+$ bond is rather strong as compared to the binding of 8a^+ to $\mathbf{1}$ or $\mathbf{1}\bullet\mathbf{1}$, this ion can be used as a reference. The remarkable growth of its relative intensity (Figure 3) indeed indicates the collision-induced destruction of the $[8\text{a}^+\bullet\mathbf{1}]$ and $[8\text{a}^+\text{@}\mathbf{1}\bullet\mathbf{1}]$ ions.



Provided that this model holds true, the most important conclusion is that much more energy is required to fragment the dimer–guest complex as compared to the monomer–guest cation. This is expected to occur for a capsule-like dimer with the guest inside the cavity but should not be observed for unspecifically bound complexes of two monomers and one ammonium ion.

^1H NMR Experiments. Independent evidence for the encapsulation of 8a^+ in dimeric $\mathbf{1}\bullet\mathbf{1}$ in solution comes from NMR experiments (Figure 4). The formation of an assembly in CDCl_3 is indicated by a downfield shift of ca. 1.1 ppm (see Experimental Section) relative to its position in $\text{DMSO}-d_6$ of the signal for the distal urea *N-H* protons. Thus, these protons are likely to be involved in hydrogen-bond formation. The *N-H* signal is

a simple singlet pointing to a symmetric complex in which all four distal *N-H* protons are equivalent. In chloroform solution, three signals for the guest inside the capsule were observed in the region of 1.0 to -1.0 ppm. The fourth signal is likely hidden under the signals for the alkyl chains. These signals can be assigned as shown in Figure 4, and they are shifted upfield by up to $\Delta\delta = 3.2$ ppm due to shielding from the aromatic capsule walls. It should be noted that the concentrations used for NMR are in the mM range, while the MS experiments were performed at μM concentrations. Due to these differences both approaches need not necessarily lead to identical results. Nevertheless, the NMR experiments provide direct evidence for the encapsulation of the charged guest in solution.

Binding Studies with $\mathbf{1}\bullet\mathbf{1}$ and Different Guests. Size and shape selectivity may serve as a further criterion for the formation of host–guest encapsulation complexes. In each series of guests—aliphatic $7^+ \text{--} 11^+$ and aromatic $12^+ \text{--} 14^+$ —the ammonium ions should have similar properties for unspecific binding to **1**. However, strict size selectivity is expected for inclusion complexes, because neither empty space within the cavity nor strain on the seam of hydrogen bonds due to large guests is favorable for the formation of the capsules in solution.³²

Before reporting the results of the binding studies, let us mention one caveat about the use of gas-phase measurements on solution-phase phenomena. Strictly speaking, mass spectrometry only reflects the properties of gas-phase species. Nevertheless, the correlation between gas phase and solution is often reliable for ESI-MS, and consequently, this method has recently been used to analyze solution-phase aggregation processes.^{16c,34} For hydrogen-bonded inclusion complexes, particular enthalpic and entropic effects may, however, play a role. Although noncompetitive solvents do not have strong interactions with the capsules and their hydrogen bonding sites, the hydrogen bonds can be expected to become stronger upon desolvation during the electrospray process.³⁵ This strengthens the assembly and slows down guest release. On the other hand, an empty capsule and a free guest are entropically favored over the inclusion complex in the gas phase, because the space available for the guest is much smaller inside the cavity. The opposite is true in solution. An empty cavity would exclude a fraction of the total space available for the guest. In solution, either a solvent molecule or a guest inside the cavity is entropically more favorable. Consequently, the transition from solution to gas phase during the electrospray process may alter the relative abundances of the different species observed in the mass spectra as compared to solution.

To determine the relative binding affinities of different guests, competition experiments were performed with all possible combinations of guests $7^+ \text{--} 14^+$ (Chart 2). Equal amounts of two guest salts were dissolved in CHCl_3 together with **1**, and the ESI mass spectra were recorded. Information about the quality of the ammonium ions as guests was directly derived from the relative signal intensities of the two capsules in each experiment (Table 1). For the reasons discussed above, these results necessarily remained qualitative in nature. Furthermore,

(34) For example, see: (a) Loo, J. A.; Ogorzalek-Loo, R. R.; Udseht, H. R.; Edmonds, C. G.; Smith, C. G. *Rapid Commun. Mass Spectrom.* **1991**, *5*, 582. (b) Guevremont, R.; Siu, K. W. M.; Le Blanc, J. C. Y.; Berman, S. S. *J. Am. Soc. Mass Spectrom.* **1992**, *3*, 216. (c) Clemmer, D. E.; Hudgins, R. R.; Jarrold, M. F. *J. Am. Chem. Soc.* **1995**, *117*, 10141.

(35) For literature dealing with hydrogen-bonding in the gas phase, see: (a) Legon, A. C.; Millen, D. J. *Chem. Rev.* **1986**, *86*, 635. (b) Legon, A. C.; Millen, D. J. *Acc. Chem. Res.* **1987**, *20*, 39. (c) Legon, A. C.; Millen, D. J. *Chem. Soc. Rev.* **1992**, 71.

Table 1. Relative Intensities for Inclusion Complexes [$G_1^+@1\bullet 1$] and [$G_2^+@1\bullet 1$] in ESI-MS Spectra (50 μM CHCl_3 Solutions of Calixarene **1** with 1 equiv of Each of the Guests G_1^+ and G_2^+)^a

G_1^+	G_2^+	I_1	I_2	G_1^+	G_2^+	I_1	I_2
7⁺	8a⁺	9	91	9⁺	11⁺	>99.5	<0.5
7⁺	9⁺	76	24	9⁺	12⁺	25	75
7⁺	10⁺	<0.5	>99.5	9⁺	13⁺	55	45
7⁺	11⁺	>99.5	<0.5	9⁺	14⁺	>99.5	<0.5
7⁺	12⁺	54	46	10⁺	11⁺	>99.5	<0.5
7⁺	13⁺	79	21	10⁺	12⁺	>99.5	<0.5
7⁺	14⁺	>99.5	<0.5	10⁺	13⁺	>99.5	<0.5
8a⁺	9⁺	97	3	10⁺	14⁺	>99.5	<0.5
8a⁺	10⁺	2	98	11⁺	12⁺	<0.5	>99.5
8a⁺	11⁺	>99.5	<0.5	11⁺	13⁺	<0.5	>99.5
8a⁺	12⁺	92	8	11⁺	14⁺	b)	
8a⁺	13⁺	97	3	12⁺	13⁺	78	22
8a⁺	14⁺	>99.5	<0.5	12⁺	14⁺	>99.5	<0.5
9⁺	10⁺	<0.5	>99.5	13⁺	14⁺	>99.5	<0.5

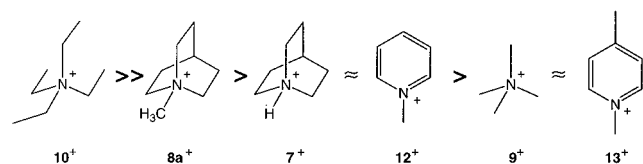
^a Intensities are normalized to $\sum(I_i) = 100\%$. ^b No signals due to the encapsulated guests are observed. Only signals for [**1**•**Na**⁺] and [**1**•**Na**⁺] are found.

Table 2. Volumes of Guests **7⁺**–**14⁺** and Packing Coefficients for Dimeric **1**•**1** (Empty Cavity: $V_C = 190 \text{ \AA}^3$) as Derived from Force Field Calculations^a

G^+	volume (\AA^3)	packing coefficient	G^+	volume (\AA^3)	packing coefficient
7⁺	110.1	0.58	11⁺	277.7	1.46
8a⁺	126.7	0.67	12⁺	92.0	0.48
9⁺	84.7	0.45	13⁺	107.6	0.57
10⁺	148.0	0.78	14⁺	195.0	1.03

^a The structures of the cavity and the guests were minimized with the Amber* force field as implemented in MacroModel 5.5.³⁰ The volumes were calculated with the GRASP program³¹ as described in ref 32.

Scheme 1



quantification of relative binding constants is impossible because the solvent is known to be a guest as well, and thus, the effective capsule concentration cannot be determined from the mass spectra.

According to the data summarized in Table 2, the best guest is **10⁺**, followed by **8a⁺** and **7⁺** (Scheme 1). **12⁺** binds nearly as well as **7⁺**, followed by **9⁺** and **13⁺**. Both **11⁺** and **14⁺**—molecules too large for the cavity of the calixarene capsule—gave no detectable signals in any of the competition experiments. These data point to encapsulation with a pronounced size selectivity. In the series of the tetraalkylammonium ions, for example, **9⁺** is too small to fill the volume of the cavity, **10⁺** seems to have the appropriate size, and **11⁺** is much too large. The shape of the guest ions is also important. Both **8a⁺** and **12⁺** have roughly the same circumferences, but the additional C_2H_4 bridge of **8a⁺** matches more closely the egg-shaped cavity of the calixarene dimer. The congruence in shape helps to maximize the van der Waals contacts with the cavity walls.

These results not only strongly support the structural assignment of the host–guest complexes but also demonstrate that the mass spectrometric approach gives ready qualitative estimates of the binding abilities of guests and of the binding properties of capsules.

In an earlier study,³² it was shown that neutral guests did not completely fill the cavities of dimeric **1** and similar capsules. Rather, a packing coefficient of ca. 0.55 was found for good guests, provided that the cavity and guests were congruous in shape. This value matches well the packing coefficients calculated for many organic solvents in their liquid states.³² For further support of the binding studies discussed above, the structures of the empty cavity of the calixarene dimer and the guests were modeled with the Amber* force field as implemented in the MacroModel 5.5 program.³⁰ On the basis of these structures, the volumes of the empty cavity (190 \AA^3) and the guests were calculated³² with the GRASP program³¹ (Table 2). Since force field calculations are not particularly accurate, we again consider these results as qualitative. Nevertheless, direct comparability of the packing coefficients reported here to those given earlier³² is ensured by applying the same computational procedures. As expected, guests **11⁺** and **14⁺**, with packing coefficients of 1.46 and 1.03, respectively, are much too large for encapsulation. It also seems reasonable that **12⁺** and **13⁺**, with packing coefficients close to 0.55, do not represent good guests because their shape poorly matches the shape of the cavity. Surprisingly, the packing coefficients of the two best guests included in this study, **8a⁺** and **10⁺**, are significantly higher than expected (0.66 and 0.78, respectively).

One may speculate that additional forces which do not play a role for neutral guest binding, such as cation– π interactions²⁶ between the guest ions and the calixarene walls, result in the higher occupancy of the capsules. Often, electrostatic attractions³⁶ between the cation and the π -systems contribute a major part of the cation– π binding energy.³⁷ Other forces such as, for example, polarizabilities generally also play a significant role but, for a given series of similar aromatic systems, make a constant contribution.³⁸ Consequently, inspection of the electrostatic potential surface of the host should provide a useful tool for the qualitative prediction of cation– π interactions.^{36,39} The calixarene capsules are rather large systems, even for a semiempirical approach to the electrostatic potential surface. Therefore, the geometry of the complete capsule [**8a⁺@1**•**1**] has been optimized with the Amber* force field first. After removal of one of the monomers, the guest, and the solubilizing groups at the molecule's periphery, a single-point calculation of calixarene **15** at the semiempirical AM1 level⁴⁰ gives the electrostatic potential surface depicted in Figure 5a. While the outer, convex surface of the calixarene is close to a neutral potential, the inner, concave surface is largely negative. Thus, electrostatically, the concave surface of the cavity provides an ideal environment for the cationic guests. Molecule **16** (Figure

(36) We follow a definition, which considers as "electrostatic" the interactions of the cation with the electrostatic field of the unpolarized molecule. Charge-induced multipole attractions are considered to be polarization interactions. For a thorough discussion, see: Dunbar, R. C. *J. Phys. Chem. A* **1998**, *102*, 8946.

(37) (a) Kearny, P. C.; Mizoue, L. S.; Kumpf, R. A.; Forman, J. E.; McCurdy, A.; Dougherty, D. A. *J. Am. Chem. Soc.* **1993**, *115*, 9907. (b) Caldwell, J. W.; Kollman, P. A. *J. Am. Chem. Soc.* **1995**, *117*, 4177. (c) Mecozzi, S.; West, A. P., Jr.; Dougherty, D. A. *J. Am. Chem. Soc.* **1996**, *118*, 2307.

(38) (a) Craven, I. E.; Hesling, M. R.; Laver, D. R.; Lukins, P. B.; Ritchie, G. L. D. *J. Phys. Chem.* **1989**, *93*, 627. (b) Gentle, I. R.; Ritchie, G. L. D. *J. Phys. Chem.* **1989**, *93*, 7740. (c) Schneider, H.-J. *Angew. Chem., Int. Ed. Engl.* **1991**, *30*, 1417. (d) Kim, K. S.; Lee, J. Y.; Lee, S. J.; Ha, T.-K.; Kim, D. H. *J. Am. Chem. Soc.* **1994**, *116*, 7399. (e) Lee, J. Y.; Lee, S. J.; Choi, H. S.; Cho, S. J.; Kim, K. S.; Ha, T.-K. *Chem. Phys. Lett.* **1995**, *232*, 67.

(39) Mecozzi, S.; West, A. P., Jr.; Dougherty, D. A. *Proc. Natl. Acad. Sci. U.S.A.* **1996**, *93*, 10566.

(40) The semiempirical calculations were conducted with the MacSpartan program package (Wavefunction Inc., 18401 Von Karman, Suite 370, Irvine, CA, 92715).

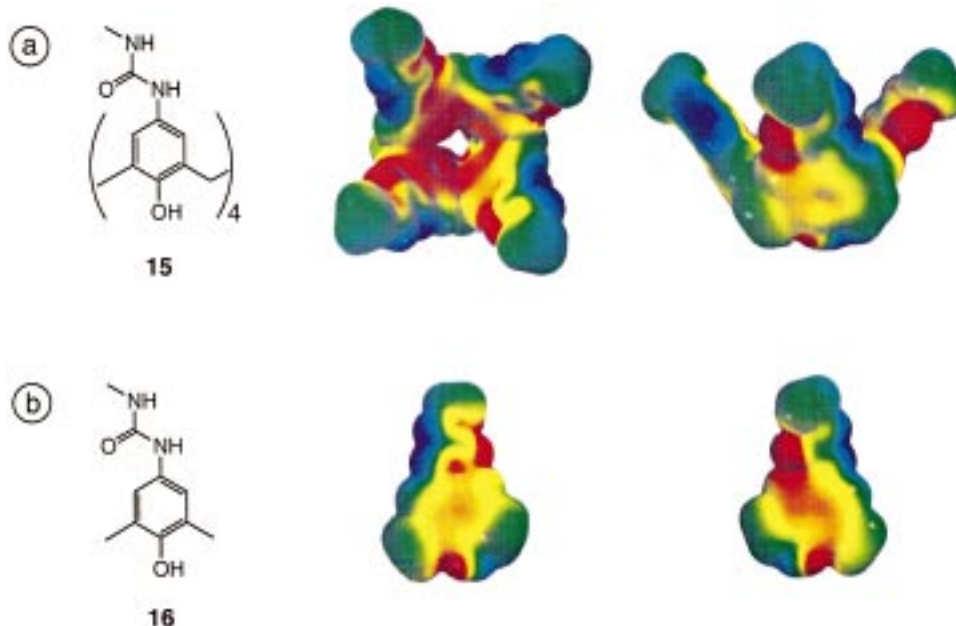


Figure 5. Semiempirically calculated electrostatic potential surfaces (AM1) of (a) calixarene **15** and (b) one of its constituent 2,6-dimethyl-4-urea phenol subunits **16** after cutting away the other three building blocks. Red parts of the molecule correspond to negative potentials (≤ -30 kcal/mol), blue parts to positive potentials (≥ 50 kcal/mol).

5b) is geometrically identical to one of the four subunits of the calixarene and has the same substitution pattern. Thus, direct comparison to **15** is possible and, in line with a recent publication on molecular tweezers,⁴¹ reveals that the negative potential on the concave surface is mainly due to the curvature of the molecule: both sides of the aromatic ring in **16** have nearly the same electrostatic potential, while this situation is drastically altered in **15**. These results point to rather strong cation- π interactions between host and guest⁴² and are in good agreement with the larger packing coefficients of charged versus neutral guests.

Heterodimer Formation. The formation of heterodimers from two different monomers has frequently been used to verify capsule formation in solution^{2d,e,21c,43} and the gas phase.⁴ Previous NMR studies^{21f,23b,44} with neutral guests revealed the exclusive formation of heterodimers from tetrakis(arylurea) calixarenes such as **1** or **2** and tetrakis(sulfonylurea) calixarene **3**. It seemed promising to test the new mass spectrometric protocol with respect to its ability to reproduce these results with ionic guest $8a^+$ and mixtures of **1** or **2** with **3**.

First, the homodimers $[8a^+@2\bullet2]$ (Figure 6a, $m/z = 3282$) and $[8a^+@3\bullet3]$ (Figure 6b, $m/z = 3794$) were characterized as host-guest assemblies as described above for $[8a^+@1\bullet1]$. An equimolar mixture of tetrakis(arylurea) calixarene **2** and tetrakis(sulfonylurea) calixarene **3** with $8a^+$ as the guest gave a clean electrospray mass spectrum with a signal for $[8a^+@2\bullet3]$ ($m/z = 3538$) as the base peak (Figure 6c). Neither of the two homodimers $[8a^+@2\bullet2]$ and $[8a^+@3\bullet3]$ could be observed in the spectrum. The same result was obtained for a mixture of **1** and **3** with $8a^+$ (Figure 6d). Again, no signals for the homodimers were found. Instead, the heterodimer $[8a^+@1\bullet3]$

($m/z = 3145$) gave rise to the base peak. A different situation was found for mixtures of the two tetrakis(arylurea) calixarenes **1** and **2** with $8a^+$ (Figure 6e). As expected, no preference for the heterodimer $[8a^+@1\bullet2]$ ($m/z = 2889$) was observed. Rather, the $[8a^+@1\bullet1]:[8a^+@1\bullet2]:[8a^+@2\bullet2]$ ratio was close to the statistical 1:2:1 distribution.⁴⁵ These findings almost exactly parallel the NMR results with neutral guests obtained previously.^{21f,23b,44}

The results presented so far—collision experiments, size and shape selectivity, control experiments with competitive solvents and labeled guests, and the formation of heterodimers which exactly parallels the behavior known for capsules with neutral guests—indicate that the complex ions observed in the mass spectra can confidently be assigned a structure of hydrogen-bonded capsules containing quarternary ammonium ions inside their cavities.

Larger Aggregates. Calixarene dimer **4** (Chart 1) represents a bridged analogue of **1•1** which has been described in a recent study.^{23c} It is not easy to distinguish intramolecular cleft-like capsule formation giving rise to $[8a^+@4]$ from intermolecular formation of, most likely, cyclic oligomers $[8a^+@4]_n$ ($n \geq 2$) by NMR experiments alone. Although these assemblies all would have the same mass-to-charge ratio of $m/z = 2902$, mass spectrometry easily provides the solution to this problem by analysis of the corresponding isotope patterns. While monocations such as $[8a^+@4]$ have isotope patterns with peak distances of $\Delta m = 1$, multiply charged species such as $[8a^+@4]_n$ show isotope separations of $\Delta m = 1/n$. In the ESI mass spectrum of **4** and $8a^+$ (Figure 7a), $[8a^+@4]$ ($m/z = 2902$) gives rise to the base peak. Comparison of the measured isotope pattern with those calculated for $[8a^+@4]$ and $[8a^+@4]_2$ (Figure 7a) reveals the assembly to be singly charged ($\Delta m = 1$), ruling out larger $[8a^+@4]_n$ ($n \geq 2$) structures and indicating intramolecular capsule formation. It should be noted that this holds true for

(41) Kamieth, M.; Klärner, F.-G.; Diederich, F. *Angew. Chem., Int. Ed.* **1998**, *37*, 3303.

(42) It is not possible to quantify this interaction for the calixarenes. For another, tetrameric capsule, a lower limit of 3.6 kcal/mol has been determined. See ref 4b.

(43) Valdés, C.; Spitz, U. P.; Toledo, L. M.; Kubik, S. W.; Rebek, J., Jr. *J. Am. Chem. Soc.* **1995**, *117*, 12733.

(44) Scheerder, J. *The Complexation of Anions by Neutral Calixarenes Derivatives*, Ph.D. thesis, University of Twente, The Netherlands, 1995.

(45) $[8a^+@1\bullet1]$, $[8a^+@1\bullet2]$, and $[8a^+@2\bullet2]$ are distributed over a large mass range ($m/z = 2495-3280$). Therefore, the deviation of the intensity ratios from the statistical 1:2:1 may be due to mass discrimination effects. Since our arguments are qualitative in nature, we did not quantify these effects for the particular instrument used.

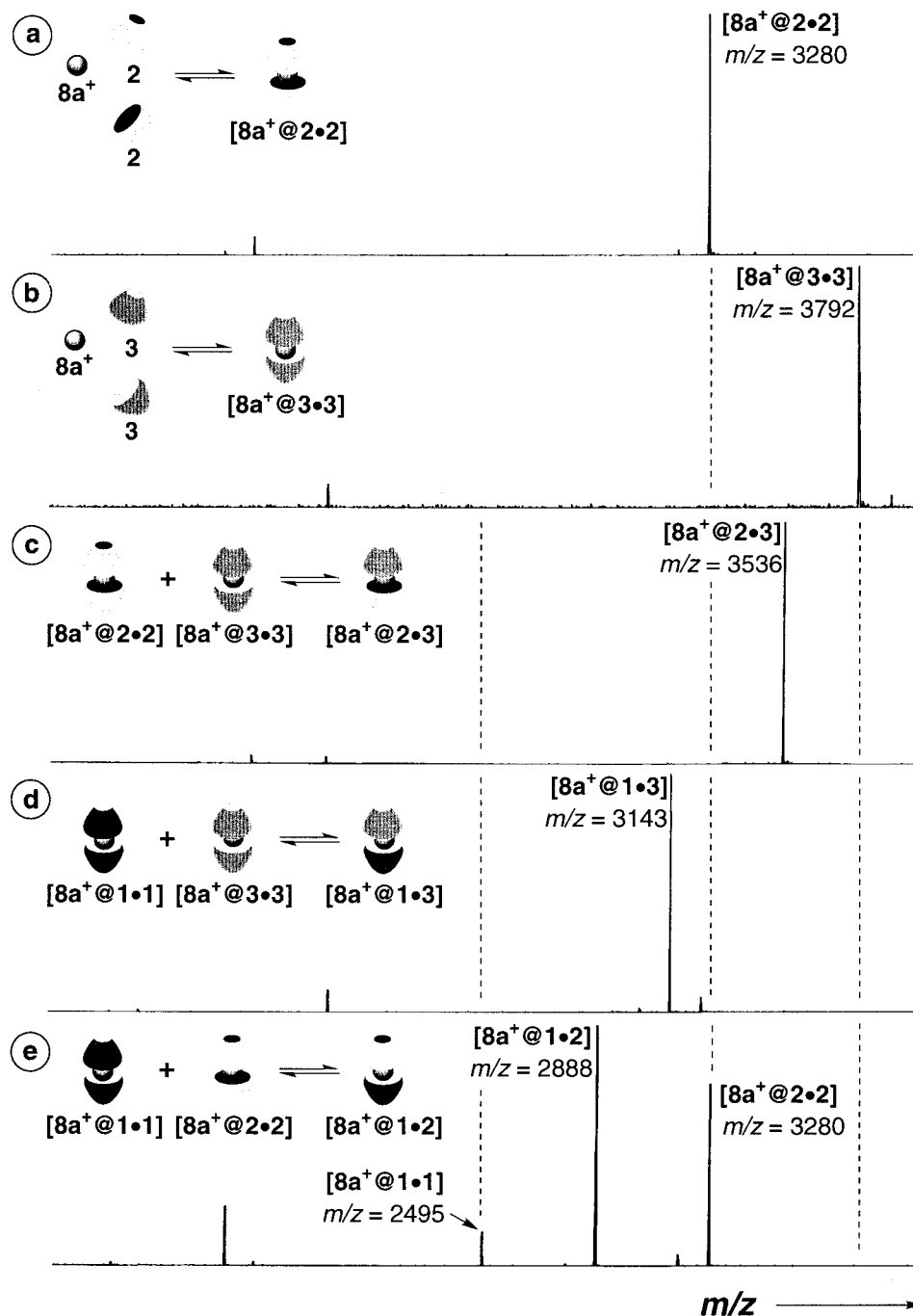


Figure 6. ESI mass spectra of CHCl_3 solutions of (a) **2** ($50 \mu\text{M}$), (b) **3** ($50 \mu\text{M}$), (c) **2** and **3** ($25 \mu\text{M}$ each), (d) **1** and **3** ($25 \mu\text{M}$ each), and (e) **1** and **2** ($25 \mu\text{M}$ each) with $8\text{a}^+ \text{BF}_4^-$ ($75 \mu\text{M}$). The dashed lines show the positions of the three homodimers $[8\text{a}^+@1\bullet1]$, $[8\text{a}^+@2\bullet2]$, and $[8\text{a}^+@3\bullet3]$ in the ESI spectra c–e.

μM concentrations as applied in these experiments. To test whether the equilibrium is shifted toward larger assemblies at higher concentrations, the concentration has been increased up to $200 \mu\text{M}$ with respect to **4**. Even at these concentrations, the isotope pattern still clearly shows the nearly exclusive presence of monocations. Adding a percentage of the isotope pattern calculated for the dication $[8\text{a}^+@4]_2$ to that of $[8\text{a}^+@4]$ reduces the fit to the experimental pattern, whatever the assumed intensity of dication.

Given the results discussed above, a 2:1 mixture of **1** and **4** with ca. 5 equiv of 8a^+ as a guest could be expected to form the homodimers $[8\text{a}^+@1\bullet1]$ and $[8\text{a}^+@4]$ as well as the dumbbell-shaped heterotrimer $[(8\text{a}^+)_2@1\bullet4\bullet1]$. However, the ESI mass spectrum of this mixture (Figure 7b) shows only

signals for homodimers $[8\text{a}^+@1\bullet1]$ ($m/z = 2495$) and $[8\text{a}^+@4]$ ($m/z = 2902$); no peak corresponding to $[(8\text{a}^+)_2@1\bullet4\bullet1]$ was detected at $m/z = 2699$. Two effects might explain this finding: (i) The intramolecular closure of **4** is entropically favored over the formation of larger structures. (ii) It is energetically unfavorable to include two positive charges within one assembly. This effect would be essentially enthalpic in nature. It should be possible to override these effects at least to some extent by addition of **3**, which should bind to **4** with enthalpy-directed preference. Indeed, in the ESI mass spectrum of a 2:1 mixture of **3** and **4** with 8a^+ as the guest (Figure 7c) an intense signal for the dumbbell $[(8\text{a}^+)_2@3\bullet4\bullet3]$ is observed at $m/z = 3348$. In contrast to the heterodimers discussed above,

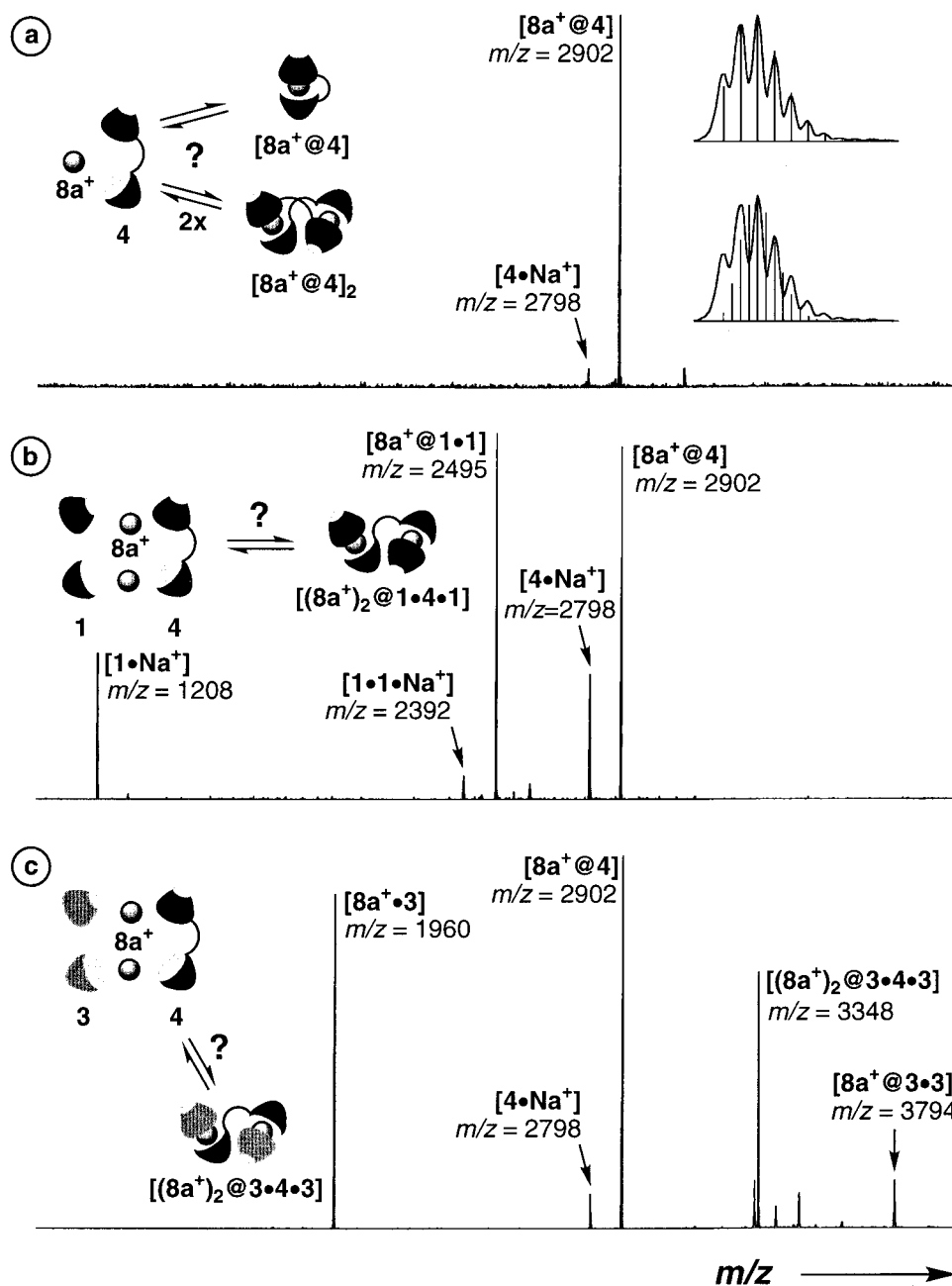


Figure 7. ESI mass spectra of (a) a CHCl_3 solution of bridged calixarene **4** ($25 \mu\text{M}$) with $8\text{a}^+ \text{BF}_4^-$ ($75 \mu\text{M}$) (the insets show the measured isotope pattern compared to those calculated for monomeric $[\text{8a}^+\text{@4}]$ and dimeric $[\text{8a}^+\text{@4}]_2$), (b) a CHCl_3 solution of **1** ($50 \mu\text{M}$) and **4** ($25 \mu\text{M}$) with $8\text{a}^+ \text{BF}_4^-$ ($250 \mu\text{M}$), and (c) a CHCl_3 solution of **3** ($50 \mu\text{M}$) and **4** ($25 \mu\text{M}$) with $8\text{a}^+ \text{BF}_4^-$ ($250 \mu\text{M}$).

the two homodimers $[\text{8a}^+\text{@4}]$ ($m/z = 2902$) and $[\text{8a}^+\text{@3•3}]$ ($m/z = 3794$) are still visible in the spectrum.

It is possible to construct dumbbell-shaped aggregates analogous to $[(\text{8a}^+)_2\text{@3•4•3}]$ with center pieces **5** and **6** (Chart 1). Figure 8a shows the ESI mass spectrum of a 2:1 mixture of **3** and **5** with 5 equiv of 8a^+ as the guest. The base peak corresponds to the adduct $[(\text{8a}^+)_2\text{@3•5•3}]$ ($m/z = 3547$). Upon encapsulation of 8b^+ , a mass shift of $\Delta m = 3$ amu is observed, as expected for a doubly charged complex which contains two guests. Further evidence for the formation of a dication comes from the signal at $m/z = 3481$, which corresponds to a chloroform molecule encapsulated within a doubly protonated dumbbell. Similarly, a very small signal was found at $m/z = 3455$ for a dumbbell containing one 8a^+ ion and one chloroform molecule. The second charge is provided by residual Na^+ . Similar complexes of low abundance have been observed for

the softballs.⁴ For monocations the distance between the two peaks should be $\Delta m = 16$. For the dications discussed here, it is only $\Delta m = 8$, as expected. The formation of $[(\text{8a}^+)_2\text{@3•5•3}]$ versus $[\text{8a}^+\text{@3•3}]$ (the latter gives rise to only a minor signal) can again be traced to the preference of tetrakis(arylurea) and tetrakis(sulfonylurea) calixarenes to form heterodimers. Furthermore, **5** is not flexible enough for intramolecular capsule formation to occur, and consequently, no signal for $[\text{8a}^+\text{@5}]$ is detected. Similarly, the calixarene trimer $[(\text{8a}^+)_3\text{@(3)_3•6}]$ ($m/z = 3768$) featuring **6** as the centerpiece corresponds to the base peak in Figure 8b. This signal is accompanied by several series of protonated and sodiated species yielding a complex spectrum.

Conclusions

Self-assembling container molecules can be readily characterized by mass spectrometry through the encapsulation of ionic

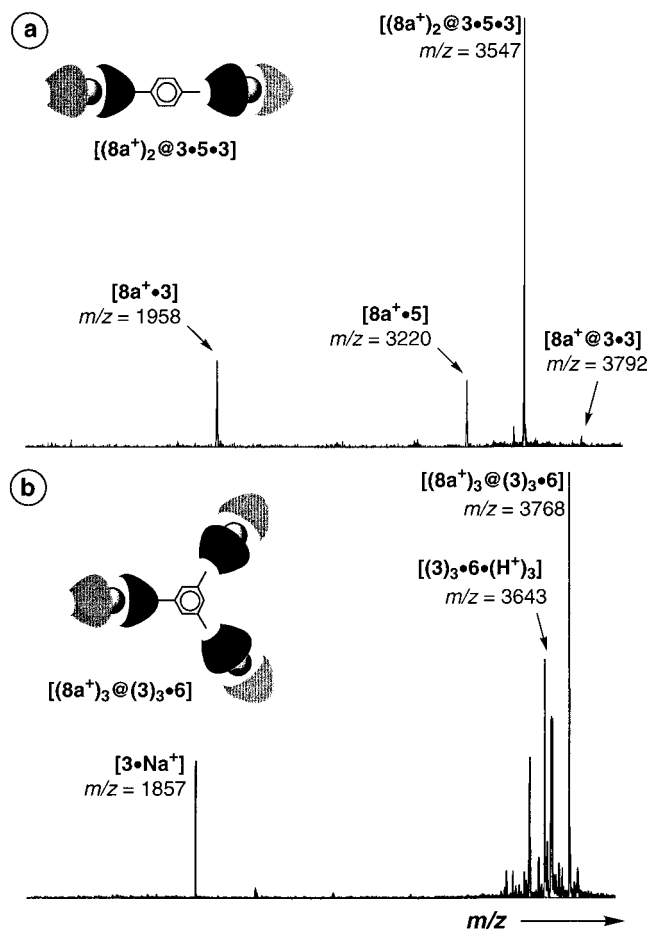


Figure 8. ESI mass spectra of (a) a CHCl_3 solution of **3** ($50 \mu\text{M}$) and **5** ($25 \mu\text{M}$) with $8\text{a}^+ \text{BF}_4^-$ ($250 \mu\text{M}$), (b) a CHCl_3 solution of **3** ($50 \mu\text{M}$) and **6** ($17 \mu\text{M}$) with $8\text{a}^+ \text{BF}_4^-$ ($750 \mu\text{M}$).

guests. The largest complexes obtained so far contain seven molecules—one centerpiece, three caps, and three guest ions—

held together by weak intermolecular forces. These structures comprise even doubly or triply charged species, extending by far the limits of mass spectrometric analysis of hydrogen-bound assemblies.

The gas-phase ion structures of these complexes have been studied by collision experiments, guest size selectivity studies, and heterodimer formation. These experiments have shown that capsules are formed in preference to unspecifically bound aggregates. The exact structures of weakly bound supramolecular aggregates are often more difficult to determine than those of covalently bound organic molecules. It may not be possible to thoroughly examine the gas-phase ion structure of other supramolecular complexes by mass spectrometry. Inclusion complexes may represent one particular case. Nevertheless, the determination of exact masses rather than average molecular weight, for example by GPC, VPO, and light scattering techniques, is advantageous and is quite generally feasible for any supramolecular complex which allows the introduction of a positive or negative charge on one of its subunits.^{4,16,18}

The mass spectrometric work discussed here complements the NMR characterization of capsules. Binding constants, for example, can easily be determined from NMR integration of signals due to encapsulated and free guest molecules. Mass spectrometry on the other hand, can more easily detect the formation of heterodimers. This will become even more important for larger capsules with lower symmetry, such as the bridged calixarene dimer **4**, which are difficult to study by NMR.

Acknowledgment. We are grateful to Professor François Diederich for helpful discussions and to Dr. Jianguye Wu and Tom Hollenbeck for technical assistance. This work was supported by the Skaggs Research Foundation and the National Institutes of Health. C.A.S. thanks the Bundesministerium für Forschung und Technologie der Bundesrepublik Deutschland and the Deutsche Akademie der Naturforscher Leopoldina (Halle/Saale) for a postdoctoral fellowship.

JA990276A